IEICE TRANS. COMMUN., VOL.E92–B, NO.6 JUNE 2009

PAPER Special Section on 3rd Pan-Pacific EMC Joint Meeting — PPEMC'08 —

FDTD Simulation Based on Spark Resistance Formula for Electromagnetic Fields due to Spark between Charged Metal Bars with Ferrite Core Attachment

Soichiro TAIRA[†], *Nonmember and* **Osamu FUJIWARA**[†a)], *Member*

SUMMARY The electromagnetic fields emitted from an electrostatic discharge (ESD) event occurring between charged metals cause seriously damage high-tech equipment. In order to clarify the generation mechanism of such ESD fields and also to reduce them, we previously proposed a finite-difference time-domain (FDTD) algorithm based on a delta-gap feeding method and a frequency dispersion characteristic formula (Naito's formula) of ferrite material for simulating the ESD fields due to a spark between the charged metals with ferrite core attachment. In the present study, by integrating the above FDTD algorithm and a spark-resistance formula, we simulated both of the ESD itself and the resultant fields for the metal bars with ferrite core attachment, and demonstrated that the core attachment close to the spark gap suppresses the magnetic field level. This finding was also validated via 6-GHz wide-band measurement of the magnetic near-field.

key words: *ESD, metal bar, ferrite core attachment, Naito's formula, spark-resistance formula, FDTD algorithm*

1. Introduction

It is well-known that the electromagnetic (EM) fields due to an electrostatic discharge (ESD) event occurring between charged metals have broadband frequency spectra over the microwave region [1], which gives serious damage to high-tech information devices.

As for the above-mentioned ESD fields, considerable efforts specifically on analytical aspects [2]–[5] have been made, while the effects of metals on the ESD fields have not been well understood. We therefore analyzed the EM fields caused by a spark discharge between spherical metals using the finite-difference time-domain (FDTD) method, which was based on gap excitation by the source of a spark current or voltage, and showed that the metals enhance the field level according to the metal dimension [6].

On the other hand, since ferrite materials have commonly been used for electromagnetic interference (EMI) countermeasures, we proposed an FDTD algorithm based on a delta-gap feeding method and a frequency dispersion characteristic formula (Naito's formula) [7] of ferrite material for investigating effects of ferrite core attachment on the ESD fields due to metal bars, and showed that the core attachment near to the spark gap suppresses the ESD filed level [8]. This finding, however, was confirmed by measuring not the magnitude of ESD fields but the detection frequencies of the electric far-field with a commercially available ESD detector, and then by demonstrating statistically that the core attachment reduces the detection distance.

In this study, by integrating our previously developed FDTD algorithm and a spark resistance formula, we simulate both of a spark between the metal bars with ferrite core attachment and the resultant ESD fields. The effect of the core attachment location on the ESD fields is examined, which is also validated from 6-GHz wide-band measurement of the ESD fields.

2. FDTD Algorithm

2.1 ESD Model

Figures 1(a) and 1(b) show an ESD model between metal bars attached by ferrite cores and its FDTD model, respectively. Two metal cylinders with length of L, whose end has a hemisphere with a radius of a, were used and they were spaced at a gap of ℓ. Two commercially available ferrite cores, of the type used frequently to counter EMI, were attached to the metal cylinders so that the central axes of the cylinders and cores correspond as shown in Fig. 1(a). They had an internal diameter of d, an outer diameter of D and a length of s. For the FDTD model shown in Fig. 1(b), the metal bars and ferrite cores were constructed by small cubic cells with a side of 0.5 mm.

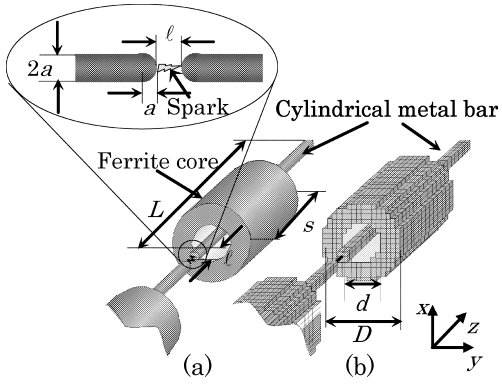

Fig. 1 (a) ESD model of cylindrical metal bars attached by ferrite cores and (b) FDTD model.

Manuscript received September 16, 2008.
Manuscript revised December 9, 2008.

[†]The authors are with the Graduate School of Engineering, Nagoya Institute of Technology, Nagoya-shi, 466-8555 Japan.
a) E-mail: Fujiwara@odin.nitech.ac.jp

DOI: 10.1587/transcom.E92.B.1960

2.2 Ferrite Core

The EM fields inside the ferrite core shown in Fig. 1 can be calculated by using the FDTD algorithm in [8], which will briefly be described in this section.

We assume that the complex relative permeability $\dot{\mu}_r$ of ferrite cores used for EMI countermeasures follows the frequency dispersion formula proposed by Naito [7], which is given as the imaginary unit of $jj = \sqrt{-1}$ by

$$\dot{\mu}(jj\omega) = \mu_0\left(1 + \frac{\mu_{rs}}{1 + jj\omega/\omega_s}\right). \tag{1}$$

Here μ_0 is the permeability of free space, μ_{rs} is the initial relative permeability related to the spin rotation motion of a ferrite core and ω_s is the spin resonance angular frequency.

In the FDTD computation, substituting Eq. (1) into the following equation:

$$\boldsymbol{B} = \dot{\mu}(jj\omega)\boldsymbol{H} \tag{2}$$

and then transforming this into the time domain, we have

$$\frac{1}{\omega_s}\cdot\frac{\partial \boldsymbol{B}}{\partial t} + \boldsymbol{B} = \frac{\mu_0}{\omega_s}\cdot\frac{\partial \boldsymbol{H}}{\partial t} + \mu_0(1+\mu_{rs})\boldsymbol{H}. \tag{3}$$

Let δ_x, δ_y, and δ_z be the sizes of the FDTD cell in x, y, and z-directions, respectively. Denoting by $\delta x = \delta y = \delta z = \delta$ the difference interval of space, and by δt the difference interval of time, we write the difference function of $W = W(x, y, z, t)$ as $W^n(i, j, k) = W(i\delta x, j\delta y, k\delta z, n\delta t)$. Assuming that a spark discharge between the cylindrical metals as shown in Fig. 1(a) occurs in the z-direction, we have the z-component of the magnetic fields, for example, which is given by

$$\begin{aligned} &H_z^{n+\frac{1}{2}}\left(i+\frac{1}{2}, j+\frac{1}{2}, k\right) \\ &= \frac{1}{1+(1+\mu_{rs}(i+\frac{1}{2}, j+\frac{1}{2}, k))\omega_s(i+\frac{1}{2}, j+\frac{1}{2}, k)\delta t} \\ &\quad\cdot\left[H_z^{n-\frac{1}{2}}\left(i+\frac{1}{2}, j+\frac{1}{2}, k\right)\right. \\ &\quad+\frac{1+\omega_s(i+\frac{1}{2}, j+\frac{1}{2}, k)\delta t}{\mu_0}B_z^{n-\frac{1}{2}}\left(i+\frac{1}{2}, j+\frac{1}{2}, k\right) \\ &\quad\left.\frac{1}{\mu_0}B_z^{n\frac{1}{2}}\left(i+\frac{1}{2}, j+\frac{1}{2}, k\right)\right] \end{aligned} \tag{4}$$

$$\begin{aligned} B_z^{n+\frac{1}{2}}\left(i+\frac{1}{2}, j+\frac{1}{2}, k\right) &= B_z^{n-\frac{1}{2}}\left(i+\frac{1}{2}, j+\frac{1}{2}, k\right) \\ &+\frac{\delta t}{\delta}\left\{E_x^n\left(i+\frac{1}{2}, j+1, k\right) - E_x^n\left(i+\frac{1}{2}, j, k\right)\right\} \\ &-\frac{\delta t}{\delta}\left\{E_y^n\left(i+1, j+\frac{1}{2}, k\right) - E_x^n\left(i, j+\frac{1}{2}, k\right)\right\}. \end{aligned} \tag{5}$$

The values of μ_{rs} and ω_s in Eq. (4) have those of the medium equivalent to each of the cells for the ferrite cores, and they thus become zero except the cells constructing the model of the ferrite cores.

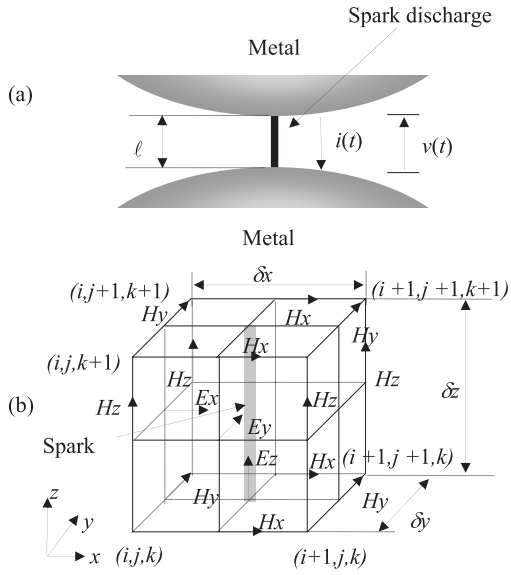

Fig. 2 (a) Spark discharge between charged metal objects and (b) arrangement of the electromagnetic field components in a spark channel.

2.3 Spark Channel

Based on a spark-resistance formula, ESD fields can be calculated from the FDTD algorithm described in [9], which will briefly be described here.

Figures 2(a) and 2(b) show a spark discharge between charged metal bodies and the FDTD model for a spark channel, respectively. Here l is the gap length, $i(t)$ the spark current at time t and $v(t)$ the spark voltage. When the spark discharge occurs between the metal bodies in the direction of z as shown in Fig. 2(b), we then have the resultant EM fields: E_x, E_y and E_z are electric fields in x, y, and z-directions, respectively, and H_x, H_y and H_z are magnetic fields in x, y, and z-directions, respectively.

Based on the Rompe-Weizel formula for a spark resistance, the time varying conductivity $\sigma(t)$ of the spark channel can be expressed as

$$\frac{\partial \sigma(t)}{\partial t} = \frac{\alpha}{p}\cdot\sigma(t)E_z(t)^2 \tag{6}$$

where p is the pressure of atmosphere that surrounds the electrical discharge part, and α is a spark constant of $\alpha = 1.1\times10^{-4}$ atm m^2/V^{2}s [9]. Discretizing Eq. (6) in terms of time and space, we have

$$\begin{aligned} &\sigma^{n+\frac{1}{2}}\left(i+\frac{1}{2}, j+\frac{1}{2}, k\right) \\ &= \frac{2+\frac{\alpha}{p}\cdot\delta t\cdot\{E_z^n(i+\frac{1}{2}, j+\frac{1}{2}, k)\}^2}{2-\frac{\alpha}{p}\cdot\delta t\cdot\{E_z^n(i+\frac{1}{2}, j+\frac{1}{2}, k)\}^2} \\ &\quad\times\sigma^{n-\frac{1}{2}}\left(i+\frac{1}{2}, j+\frac{1}{2}, k\right) \end{aligned} \tag{7}$$

where δt is the time step, and then the difference function of

the electric field E_z in the spark channel is given by

$$E_z^n\left(i+\frac{1}{2},j+\frac{1}{2},k\right)=E_z^{n-1}\left(i+\frac{1}{2},j+\frac{1}{2},k\right)\times\frac{2\varepsilon(i+\frac{1}{2},j+\frac{1}{2},k)-\delta t\sigma^{n+1/2}(i+\frac{1}{2},j+\frac{1}{2},k)}{2\varepsilon(i+\frac{1}{2},j+\frac{1}{2},k)+\delta t\sigma^{n+1/2}(i+\frac{1}{2},j+\frac{1}{2},k)}+\frac{1}{\delta}\times\frac{\delta t}{2\varepsilon(i+\frac{1}{2},j+\frac{1}{2},k)+\delta t\sigma^{n+1/2}(i+\frac{1}{2},j+\frac{1}{2},k)}\times\left[H_y^{n-1/2}\left(i+1,j+\frac{1}{2},k\right)-H_y^{n-1/2}\left(i,j+\frac{1}{2},k\right)+H_x^{n-1/2}\left(i+\frac{1}{2},j,k\right)-H_x^{n-1/2}\left(i+\frac{1}{2},j+1,k\right)\right]. \quad (8)$$

Here $\varepsilon(i,j,k)$ and $\sigma(i,j,k)$ are the permittivity and conductivity, respectively, which have numerical values corresponding to the medium of the cell.

The spark discharge was simulated separately in the process of charging and discharge. For the charging step, we injected a Gaussian pulse current $i(t)$ through the gap to reach the steady voltage between the metal objects, which also enables one to calculate the EM fields in space. For the discharge step, denote by I_s the charging current when the charge finished, and by V_s the breakdown voltage when the gap breakdown happened at time $t = 0$, corresponding to the steady voltage in the charging process. Then the initial conductivity and initial electric field inside the channel are given by $l/\delta^2 \times I_s/V_s$ and V_s/l, respectively. Based on Eq. (7) with these initial values, the spark discharge occurring between the metal bars can be simulated, which enables one to calculate the EM fields in space.

2.4 Computation Region

Figure 3 shows the FDTD computation region and arrangement of cylindrical metal bars. The region consisted of $320 \times 113 \times 505$ cubic cells with $\delta = 0.5$ mm. The following three cases for the FDTD model were considered: the first model without ferrite cores, the second and third models with the ferrite cores attached to the near end and to the far end of the gap, respectively. Twelve perfectly reflected layers were used to absorb outgoing scattered waves for simulating an open space.

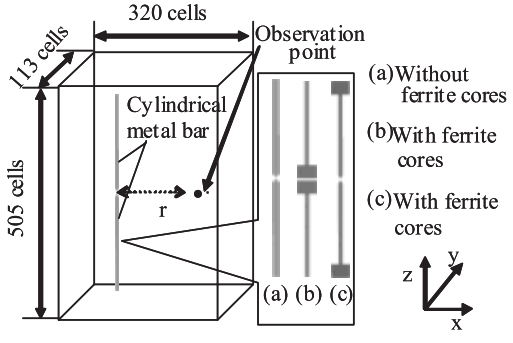

Fig. 3 Computation region and arrangement of FDTD model.

3. Experimental Validation

3.1 Setup and Method

In order to validate the above-mentioned FDTD algorithm and also to examine the effect of the ferrite core attachment on the ESD fields, in a simple spark experiment as shown in Fig. 1(a), we measured the magnetic field due to the spark, and then compared the result with the FDTD calculation.

Figure 4 shows an experimental set up. An ignition coil driven by an electronic circuit generated a high voltage, which was led to metal bars through carbon strings (250 Ω/cm) with a length of 60 cm. All these devices were set up on a wooden desk with a height of 0.8 m from the floor as shown in Fig. 4. In order to measure the transient magnetic field due to a spark discharge between the metal bars, a shielded loop antenna was placed at a distance of r = 10 cm from the spark gap, and the loop face was set horizontally to the plane including the spark direction. This loop antenna consists of a copper wire with an outside diameter of 1.2 mm, and has a loop radius of 5 mm, a loop area of S = 78.5 mm^2 and an inductance of L_c = 13.8 nH, whose output terminal was connected to a wide-band digital oscilloscope with an input impedance of Z_i = 50 Ω, a band-width of f_c = 6 GHz and a sampling frequency of 20 GHz. The breakdown voltage V_S was simultaneously measured through a high voltage probe with a digital phosphor oscilloscope with a bandwidth of 500 MHz.

As for the material of the cylindrical metal bar, brass with a conductivity of 2.0×10^7 S/m was used. The size was taken as a radius of a = 2 mm and a length of L = 10 cm. A ferrite core with an internal diameter of d = 8 mm and an outer diameter of D = 16 mm and a length of s = 14 mm was used. The intrinsic properties of the core for FDTD simulation were taken as μ_{rs} = 853, $\omega_s = 7.23 \times 10^7$ rad/s and a relative permittivity of 12. In addition, the output voltage $v_0(t)$ of the loop antenna was calculated in the following way. Figure 5 shows an FDTD model of a shielded loop antenna and its configuration. The shielded loop antenna was simulated as the same sized metal loop model with one cell gap, in which a lumped resistance of 50 Ω was inserted. For the output voltage observed through the shielded loop

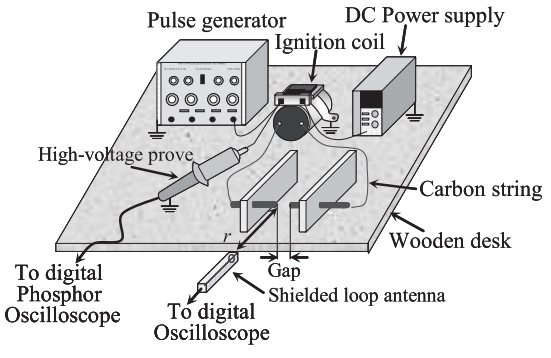

Fig. 4 Experimental set up.

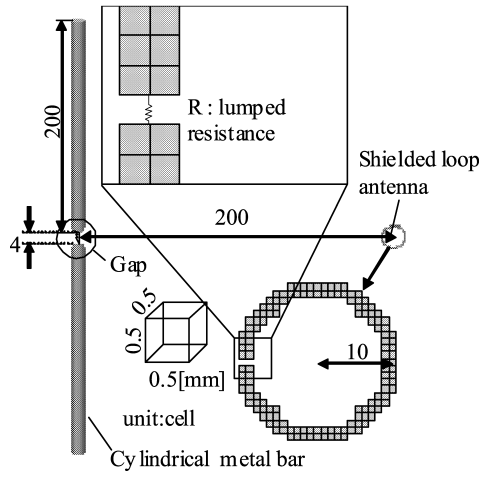

Fig. 5 FDTD model for shielded loop antenna.

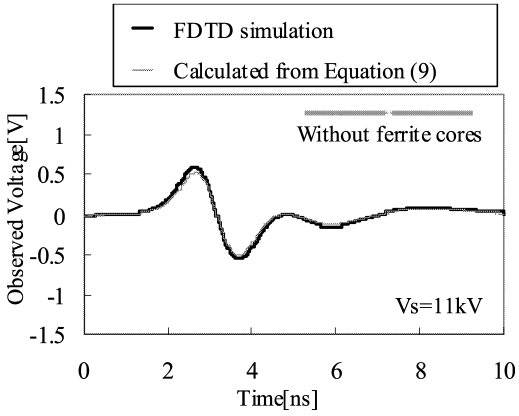

Fig. 6 Waveform observed through a shielded loop antenna (observation point: r = 10 cm; gap length: 2.0 mm).

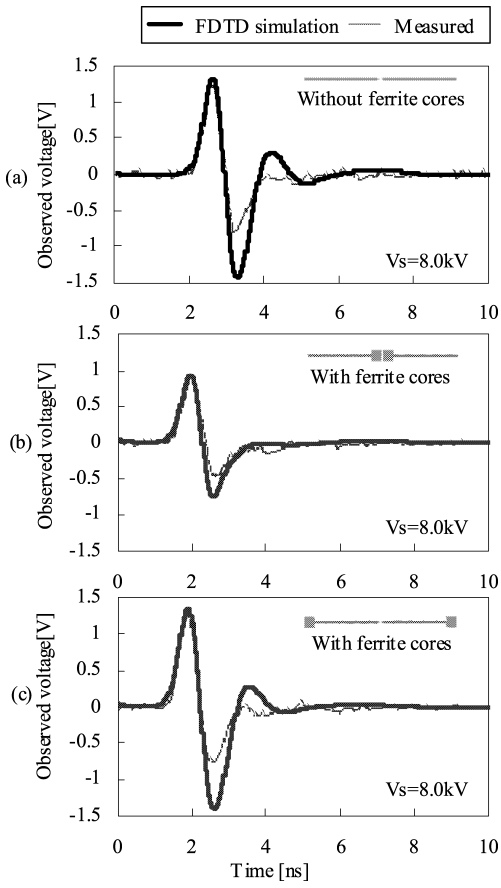

Fig. 7 Observed waveforms of transient magnetic field with a shielded loop antenna when a spark discharge between cylindrical metals occurs (observation point: r = 10 cm; gap length: 1.0 mm).

antenna, we calculated the voltage induced across the 50-Ω lumped resistance.

3.2 Results and Discussion

In order to validate the metal loop modeling of the shielded loop antenna, we simulated the voltage induced across the 50-Ω lumped resistance of the metal loop model for a spark discharge with a voltage of V_s = 11 kV occurring between cylindrical metals with a gap length of 2 mm and without ferrite core attachment, whose arrangement is shown in Fig. 5. The result was compared with the output voltage $v_0(t)$ calculated from

$$v_0(t) = -\frac{Z_i}{L_c} \times \int_0^t \frac{\partial S \mu_0 H_\phi(\xi)}{\partial \xi} \cdot \exp\left\{-\frac{Z_i}{L_c} \cdot (t-\xi)\right\} d\xi, \qquad (9)$$

where Z_i (= 50 Ω) is the input impedance of the oscilloscope and S is the loop area. $H_\phi(t)$ is the magnetic field component interlinked to the loop face.

Figure 6 shows the simulated waveform of the voltage induced across the 50-Ω lumped resistance with a thick line. Also shown with a thin line was the waveform of the output voltage $v_0(t)$ calculated from Eq. (9) where $H_\phi(t)$ was simulated. It was found that the simulated waveform agrees well with the calculated one, which ensured the validity of the metal loop model for the shielded loop antenna used in this measurement. Figure 7 shows the voltage waveforms observed through the shielded loop antenna for a spark discharge with a gap length of 1 mm. Figure 8 also shows the result for a spark discharge with a gap length of 2 mm. The thick and thin lines are the simulated and measured results, respectively. It should be noted that the first peaks in Fig. 7 (gap length: 1.0 mm) are higher than those in Fig. 8 (gap length: 2.0 mm), which may be because the smaller the spark gap length is, the larger the spark conductivity becomes [5].

We found from these figures that the FDTD algorithm approximately simulates the first peak voltages due to the spark between the metal bars with ferrite core attachment, though there are some differences between the simulation and measurement around the second peak voltages, and also that the core attachment close to the gap end reduces the peak, while the far-end attachment does not almost affect the voltage waveform. The discrepancies around the second peak voltages may be due to other types of discharges like arcs or abnormal glow discharges following the spark [10], which can not be simulated from the present FDTD algo-

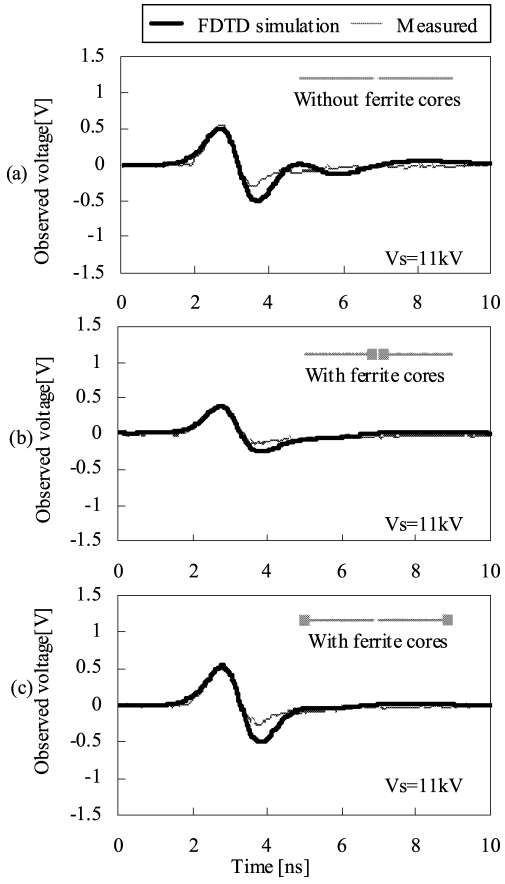

Fig. 8 Observed waveforms of transient magnetic field with a shielded loop antenna when a spark discharge between cylindrical metals occurs (observation point: r = 10 cm; gap length: 2.0 mm).

rithm.

4. Conclusion

By integrating a spark-resistance formula and our previously proposed FDTD algorithm based on Naito's formula of ferrite material, we simulated both of ESD itself and the resultant magnetic near-field due to the spark between charged metal bars with an attachment of EMI ferrite cores. As a result, we could confirm that the proposed FDTD algorithm enables one to simulate the ESD event in this case, and that the attachment of the ferrite core to the near end of the spark gap is effective in suppressing the ESD fields.

Future subjects are to examine the suppression effects of ESD fields due to ferrite core attachment with respect to intrinsic core properties, and also to elucidate their generation mechanism. Furthermore, FDTD algorithms applicable for other types of discharges except sparks should be investigated.

References

[1] W.D. Greason, "Indirect effect of ESD: Modeling and measurement," Proc. 11th International Zurich Symposium on EMC, 116R1, pp.613–618, March 1995.

[2] P.F. Wilson and M.T. Ma, "Field radiated by electrostatic discharges," IEEE Trans. Electromagn. Compat., vol.33, no.1, pp.10–18, Feb. 1991.

[3] S. Ishigami and I. Yokoshima, "Measurements of fast transient electric fields in the vicinity of short gap discharges," Proc. 1994 International Symposium on Electromagnetic Compatibility, pp.90–93, May 1994.

[4] D. Pommerenke and M. Aidam, "ESD: Waveform calculation, field and current of human and simulator ESD," J. Electrostatics, vol.38, pp.33–51, 1996.

[5] O. Fujiwara, "An analytical approach to model indirect effect caused by electrostatic discharge," IEICE Trans. Commun., vol.E79-B, no.4, pp.483–489, April 1996.

[6] O. Fujiwara, K. Kawaguchi, and N. Kurachi, "FDTD computation modeling for electromagnetic fields generated by spark between charged metals," Proc. 14th International Wroclaw Symposium on EMC, pp.267–271, Wroclaw, Poland, 1998.

[7] Y. Naito, "On the frequency dispersion of the permeability of spinnel type ferrite," IECE Trans., vol.56, no.2, pp.113–120, Feb. 1973.

[8] O. Fujiwara and K. Kawaguchi, "A FDTD analysis of electromagnetic fields caused by electrostatic discharge between metals with ferrite material attachments," IEEJ Trans. EIS, vol.120-C, no.12, pp.1913–1919, Dec. 2000.

[9] O. Fujiwara, H. Seko, and Y. Yamanaka, "FDTD computation of electromagnetic fields due to electrostatic discharge using a spark resistance formula," IEICE Trans. Commun. (Japanese Edition), vol.J85-B, no.9, pp.1644–1651, Sept. 2002.

[10] Y. Taka, Y. Kagawa, and O. Fujiwara, "Measurement of discharge currents due to human-ESD," Proc. 2007 4th International Symposium on EMC, pp.43–46, Qingdao, China, 2007.

Soichiro Taira received his B.E. and M.E. degrees in 2003 and in 2005, respectively, from Nagoya Institute of Technology, Nagoya, Japan. He is now working for Toyota Motor Corporation.

Osamu Fujiwara received his B.E. degree in Electrical Engineering from Nagoya Institute of Technology, Nagoya, Japan in 1971, and his M.E. and D.E. degrees in electrical engineering from Nagoya University, Nagoya, Japan, in 1973 and in 1980, respectively. From 1973–1976, he worked in the Central Research Laboratory, Hitachi, Ltd., Kokubunji, Japan, where he was engaged in research and development of system packaging design for computers. From 1980 to 1984 he was with the Department of Electrical Engineering Nagoya University. In 1984 he joined the Department of Electrical and Computer Engineering, Nagoya Institute of Technology. Dr. Fujiwara is currently a professor of the Department of Computer Science and Engineering, Graduate School of Engineering, Nagoya Institute of Technology. His research interests include measurement and control of electromagnetic interference due to discharges, bioelectromagnetics, and other related EMC areas. He received Paper Awards from the IEE of Japan and the IEICE in 1980 and 2000, respectively. He also serves as an Associate Editor of the IEEE Transactions on EMC. Dr. Fujiwara is a member of the IEEE and the IEE of Japan.